Available online www.worldscientificnews.com

World Scientific News

An International Scientific Journal

WSN 211 (2026) 298-310 EISSN 2392-2192

Novel Azo-Ester Liquid Crystals: Synthesis and Mesomorphic Properties of 2-[(4′-N-Alkoxy-3′-Methoxybenzoyl)Oxy]Naphthylazo-2″-Methoxybenzenes

Jaimin G. Patel[1], **Dr. Vipul R. Patel**[2]

[1,2] Sheth P.T. Arts and Science College - Godhra, Gujarat, India.

pateljaimin5035@gmail.com, vrp181968@gmail.com

https://doi.org/10.65770/NXQE8406

ABSTRACT

A novel homologous series of thermotropic liquid crystalline azo-esters, (2-(4’-n-alkoxy-3’-methoxybenzoyloxy)-naphthylazo-2”-methoxybenzenes) (C_1-C_{18}), has been synthesized via a three step pathway involving Williamson ether synthesis, diazotization, and Steglich esterification. Comprehensive characterization using ^{1}H NMR, FTIR, mass spectrometry, and elemental analysis confirmed molecular structures. Mesomorphic properties were systematically investigated using polarized optical microscopy and differential scanning calorimetry. Compounds C_7-C_{18} exhibit well defined liquid crystalline behavior, with C_7-C_{12} displaying dual nematic-smectic polymorphism. Nematic clearing temperatures range from 159-177°C, while smectic transitions occur at 126-152°C, with mesophase ranges spanning 17-51°C. The synergistic effects of naphthalene cores (enhanced π-π stacking), azo linkages (molecular rigidity), ester connections (thermal stability), and methoxy lateral substituents (dipolar interactions) contribute to the robust mesomorphic behavior. This study establishes fundamental structure property relationships for multi ring azo ester mesogens and provides molecular design principles for advanced liquid crystalline materials with applications in display technologies and photonic devices.

Keywords: Liquid crystals, Azo compounds, Ester linkage, Mesomorphism, Thermal analysis.

(Received 11 November 2025; Accepted 21 December 2025; Date of Publication 22 January 2026)

1. INTRODUCTION

Liquid crystals (LCs) represent a unique mesomorphic state between crystalline solids and isotropic liquids, exhibiting both fluidity and long-range molecular order. This intermediate state responds sensitively to temperature, electric fields, and molecular interactions, forming the basis for modern display technologies and photonic applications. Thermotropic liquid crystals undergo temperature-driven phase transitions and are classified by molecular architecture into calamitic (rod-like), discotic (disk-like), and bent-core mesogens. Calamitic mesogens, featuring elongated aromatic cores and flexible terminal chains, exhibit diverse mesophases including nematic (N) and smectic phases. The nematic phase displays orientational order without positional ordering, while smectic phases organize into layered structures with varying degrees of in-layer order[1,2].

Rational design of high-performance liquid crystalline materials requires understanding key molecular features: rigid aromatic cores for anisotropy and π-π stacking, flexible alkyl/alkoxy chains to modulate thermal properties, and lateral substituents for fine tuning intermolecular interactions. Multi ring aromatic cores enhance clearing temperatures and broaden mesophase ranges through increased polarizability[3-6]. Linking groups such as ester (-COO-) and azo (-N=N-) functionalities critically influence molecular conformation and electronic distribution. Terminal alkyl chain length systematically affects mesomorphic behavior: short chains (C_1-C_6) typically fail to induce stable mesophases due to insufficient van der Waals interactions; medium chains (C_7-C_{14}) optimize mesophase stability; longer chains (C_{15}+) may reduce clearing temperatures. Lateral methoxy substituents introduce dipolar character while maintaining molecular linearity, thereby enhancing mesophase stability through dipole-dipole associations. Azo groups provide rigid, linear linkages and enable photochemical responsiveness through reversible trans-cis photoisomerization, opening possibilities for light switchable devices. Ester linkages contribute thermal stability and synthetic versatility, particularly through Steglich esterification methodology [7-8].

Naphthalene based mesogens offer enhanced molecular anisotropy and extended π-conjugation compared to simple benzene systems, yielding higher clearing temperatures, broader mesophase ranges, and increased propensity for smectic phase formation. The combination of naphthalene cores with azo and ester functionalities represents a promising but underexplored molecular architecture. Despite advances in liquid crystal science, predictive design of multifunctional mesogens with specific phase sequences and transition temperatures remains challenging. Current applications demand materials with enhanced thermal stability, broad operating temperature ranges, and functional responsiveness [9-12].

Systematically investigated the influence of alkyl chain length, naphthalene integration, azo linkages, and methoxy lateral substitution on mesomorphic properties using polarized optical microscopy (POM), differential scanning calorimetry (DSC), and comprehensive spectroscopic characterization (^{1}H NMR, FTIR, mass spectrometry, elemental analysis) [13-16]. This work establishes fundamental structure-property relationships for multi-ring azo-ester liquid crystals and provides molecular design principles for advanced mesogenic materials with applications in display technologies and photonic devices [17].

2. EXPERIMENTAL STUDIES

2.1. Materials and Instrumentation

All chemicals and reagents were procured from commercial suppliers and used as received unless otherwise specified. 4-Hydroxy-3-methoxybenzoic acid (vanillic acid, 98%), n-alkyl bromides (C1-C18, 95-99%), potassium hydroxide (analytical grade), 2-methoxyaniline (98%), β-naphthol (99%), sodium nitrite (99%), N,N′-dicyclohexylcarbodiimide (DCC, 99%), 4-(dimethylamino)pyridine (DMAP, 99%), and hydrochloric acid (37%) were obtained from Loba Chemie Pvt. Ltd., India. Dichloromethane and methanol were purified by standard methods and dried over molecular sieves before use.

Fourier-transform infrared (FTIR) spectra were recorded on a Shimadzu 8400 ATR spectrophotometer in the range 400-4000 cm^{-1}. ^1H NMR spectra were obtained on a JEOL 400 MHz spectrometer using $CDCl_3$ as solvent and TMS as internal standard. Mass spectra were recorded on a Shimadzu QP1000EX instrument using electron impact ionization. Elemental analysis was performed on a Carlo Erba EA 1108 analyzer.

Mesomorphic properties were investigated using polarized optical microscopy (POM) on a PW-BK 5000 PR microscope equipped with a hot stage (HS-400) and crossed polarizers. Thermal transitions were measured by differential scanning calorimetry (DSC) using a LINSIS STAPT-1000 instrument under nitrogen atmosphere with heating/cooling rates of 5°C/min.

2.2. Synthetic Procedures

2.2.1. Synthesis of 4-n-Alkoxy-3-methoxybenzoic acids (Int-A):

4-Hydroxy-3-methoxybenzoic acid (5.0 g, 29.8 mmol) was dissolved in methanol (100 mL) in a round-bottom flask equipped with a reflux condenser. Potassium hydroxide (4.2 g, 74.5 mmol) was added, followed by the appropriate n-alkyl bromide (41.7 mmol). The reaction mixture was heated under reflux for 8-12 hours with stirring. Progress was monitored by TLC (ethyl acetate:hexane 1:1). After cooling, 10% aqueous KOH (50 mL) was added, and the mixture was poured into ice-cold water (300 mL). The resulting precipitate was filtered, washed with cold water, and recrystallized from ethanol to give pure 4-n-alkoxy-3-methoxybenzoic acids in 78-85% yields[18-21].

2.2.2. Synthesis of 2-Hydroxy-naphthylazo-2′-methoxybenzene (Int-B):

2-Methoxyaniline (3.0 g, 24.4 mmol) was dissolved in water (50 mL) and concentrated HCl (10 mL) in a 500 mL beaker. The mixture was cooled to 0-5°C in an ice bath. A solution of sodium nitrite (1.85 g, 26.8 mmol) in water (25 mL) was added dropwise with continuous stirring, maintaining the temperature below 5°C. After stirring for 1 hour, a solution of β-naphthol (3.5 g, 24.4 mmol) and sodium hydroxide (2.0 g) in water (100 mL) was added slowly. The reaction mixture was stirred for 2 hours, and the resulting orange precipitate was filtered, washed with water, and recrystallized from ethanol. Yield: 91.2%[22].

2.2.3. Synthesis of Series-1 (2-(4’-n-alkoxy-3'-methoxybenzoyloxy)-naphthylazo-2”-methoxybenzenes):

In a 250 mL single neck round bottom flask (RBF), the 4-n-alkoxy-3-methoxy benzoic acid (Int-A) (1 equivalent) was dissolved in appropriate amount of dichloromethane (DCM) solvent. After that, stir the reaction mixture for an hour at room temperature while adding DCC (1.2 equivalent) and a pinch of DMAP. 2-hydroxy-naphthyl-azo-2'-methoxybenzene [Int-B] (1 equivalent) was then added, and the mixture was stirred for 24 hours at room temperature. TLC use for reaction monitoring. Following reaction completion, the solution was carefully filtered using vacuum filtration to remove the DCU precipitate, and the solvent was evaporated using a rotary evaporator. Ethanol recrystallized the crude product. The synthetic pathway is shown in Scheme 1[23].

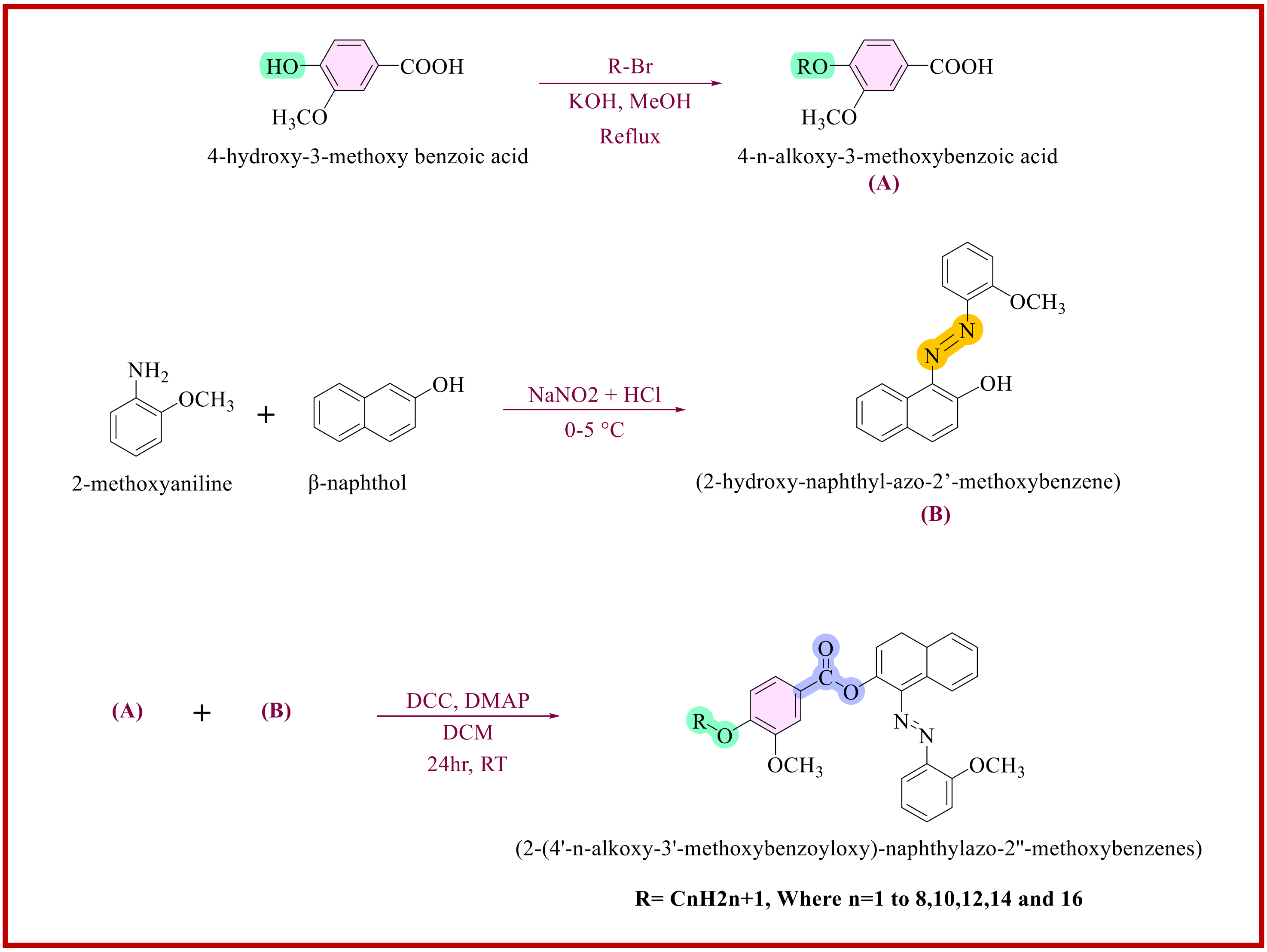

Scheme 1. Synthesis route of novel Series-1 (2-(4'-n-alkoxy-3'-methoxybenzoyloxy)-naphthylazo-2"-methoxybenzenes).

3. SYNTHESIS AND CHARACTERIZATION

The target compounds were successfully synthesized via a three-step synthetic route involving Williamson ether synthesis, diazotization-coupling reaction, and Steglich esterification. The overall yields ranged from 65-78% for the final products. All intermediates and final compounds were characterized by spectroscopic methods and showed excellent agreement with the proposed structures.

3.1. Spectroscopic Characterization

3.1.1. IR Spectral Analysis

Decyloxy derivative (C10):

The IR spectrum showed characteristic peaks at 720-770 cm^{-1} (C-H of polymethylene groups, $-C_{10}H_{21}$), 830-850 cm^{-1} (para-disubstituted benzene ring), 1100-1300 cm^{-1} (C-O-C stretching of alkoxy group), 1600-1650 cm^{-1} (N=N azo stretching and aromatic C=C), 1650-1750 cm^{-1} (C=O stretching of ester group), and 2850-2950 cm^{-1} (C-H stretching of alkyl chain). IR consistent with the proposed structure.

Dodecyloxy derivative (C12):

The IR spectrum exhibited peaks at 644-742 cm^{-1} (-(CH$_2$)n- of dodecyloxy chain), 830 and 864 cm^{-1} (para-disubstituted benzene ring), 1100-1300 cm^{-1} (C-O-C stretching of alkoxy group), 1547, 1593, and 1612 cm^{-1} (N=N azo stretching and aromatic C=C), 1640-1665 cm^{-1} (aromatic C=C stretching), 1713 cm^{-1} (C=O stretching of ester group), 2851 and 2921 cm^{-1} (C-H stretching of aliphatic chains), and 3010 cm^{-1} (aromatic C-H stretching). IR consistent with the proposed structure.

3.1.2. ^{1}H NMR Spectral Analysis

Hexyloxy derivative (C6):

^{1}H NMR (400 MHz, CDCl$_3$, δ ppm): 0.83-0.88 (t, 3H, -CH$_3$ of hexyloxy chain), 1.25-1.62 (m, 6H, -CH$_2$- of hexyloxy chain), 1.76-1.84 (m, 2H, -OCH$_2$-CH$_2$- adjacent to oxygen), 3.89-3.97 (s, 6H, -OCH$_3$ groups), 4.04-4.16 (t, 2H, -OCH$_2$- of hexyloxy chain), 6.78-7.67 (m, aromatic protons of benzene and naphthalene rings), 7.94-8.52 (m, aromatic protons ortho to azo and ester groups).

The ^{1}H NMR data confirms the presence of hexyloxy chain, methoxy substituents, ester linkage, and azo-aromatic system, consistent with the proposed structure.

Dodecyloxy derivative (C12):

^{1}H NMR (400 MHz, CDCl$_3$, δ ppm): 0.76-0.81 (t, 3H, -CH$_3$ of dodecyloxy chain), 1.15-1.36 (m, 18H, -CH$_2$- of dodecyloxy chain), 1.70-1.77 (m, 2H, -OCH$_2$-CH$_2$- adjacent to oxygen), 3.73-3.97 (s, 6H, -OCH$_3$ groups), 4.16-4.18 (t, 2H, -OCH$_2$- of dodecyloxy chain), 6.68-7.57 (m, aromatic protons), 7.94-8.41 (m, aromatic protons ortho to azo and ester groups).

The ^{1}H NMR data confirms the presence of dodecyloxy chain, methoxy substituents, ester linkage, and azo-aromatic system, consistent with the proposed structure.

3.1.3. Mass Spectral Analysis

Dodecyloxy derivative (C12):

m/z (rel. int%): 572 (M$^+$, molecular ion peak), 231 (base peak), 214, 189, 147, 127, 119, 91, 65.

The molecular ion peak at m/z 572 confirms the molecular formula, and fragmentation pattern supports the proposed structure.

3.1.4. Elemental Analysis

The synthesized liquid crystalline compounds of the (2-(4’-n-alkoxy-3’-methoxybenzoyloxy)-naphthylazo-2’’-methoxybenzenes) series were analyzed for elemental composition (CHN analysis). The experimental data obtained are in good agreement with the theoretical values calculated for the corresponding compounds.

Table 1. Elemental analysis

Sr. no	R= n-alkyl group	Molecular Formula	Elements % Found (% Calculated)		
			C	H	N
1	C1	$C_{26}H_{22}N_2O_5$	70.58(70.61)	5.01(5.03)	6.33(6.37)
2	C2	$C_{27}H_{24}N_2O_5$	70.58(70.59)	5.01(5.04)	6.33(6.36)

3	C3	$C_{28}H_{26}N_2O_5$	71.04(71.01)	5.30(5.28)	6.14(6.17)
4	C4	$C_{29}H_{28}N_2O_5$	71.47(71.51)	5.57(5.54)	5.95(5.91)
5	C5	$C_{30}H_{30}N_2O_5$	72.27(72.24)	6.06(6.02)	5.62(5.58)
6	C6	$C_{31}H_{32}N_2O_5$	72.64(72.68)	6.29(6.33)	5.47(5.51)
7	C7	$C_{32}H_{34}N_2O_5$	72.98(73.02)	6.51(6.55)	5.32(5.36)
8	C8	$C_{33}H_{36}N_2O_5$	73.31(73.33)	6.71(6.75)	5.18(5.21)
9	C10	$C_{34}H_{38}N_2O_5$	73.62(73.63)	6.90(6.89)	5.05(5.01)
10	C12	$C_{35}H_{40}N_2O_5$	73.92(73.93)	7.09(7.10)	4.93(4.95)
11	C14	$C_{37}H_{44}N_2O_5$	74.47(74.51)	7.43(7.44)	4.69(4.72)
12	C16	$C_{39}H_{48}N_2O_5$	74.97(75.95)	7.74(7.76)	4.48(4.52)
13	C18	$C_{41}H_{52}N_2O_5$	75.43(75.47)	8.03(8.01)	4.29(4.33)

4. RESULTS AND DISCUSSION

4.1. Mesomorphic Properties

The mesomorphic behavior of the synthesized compounds was comprehensively studied using POM and DSC analysis. The transition temperatures are summarized in Table 2.

Table 2. Transition temperatures (°C) on heating cycle.

Sr	R= n-alkyl group	Transition temperatures in °C		
		Smectic	Nematic	Isotropic
1	C1	-	-	180
2	C2	-	-	180
3	C3	-	-	178
4	C4	-	-	179
5	C5	-	-	177
6	C6	-	-	170

7	C7	126	143	177
8	C8	(128)	146	175
9	C10	(147)	151	176
10	C12	148	156	175
11	C14	152	-	166
12	C16	140	-	159

( ) indicates monotropy; Sm = Smectic, N = Nematic

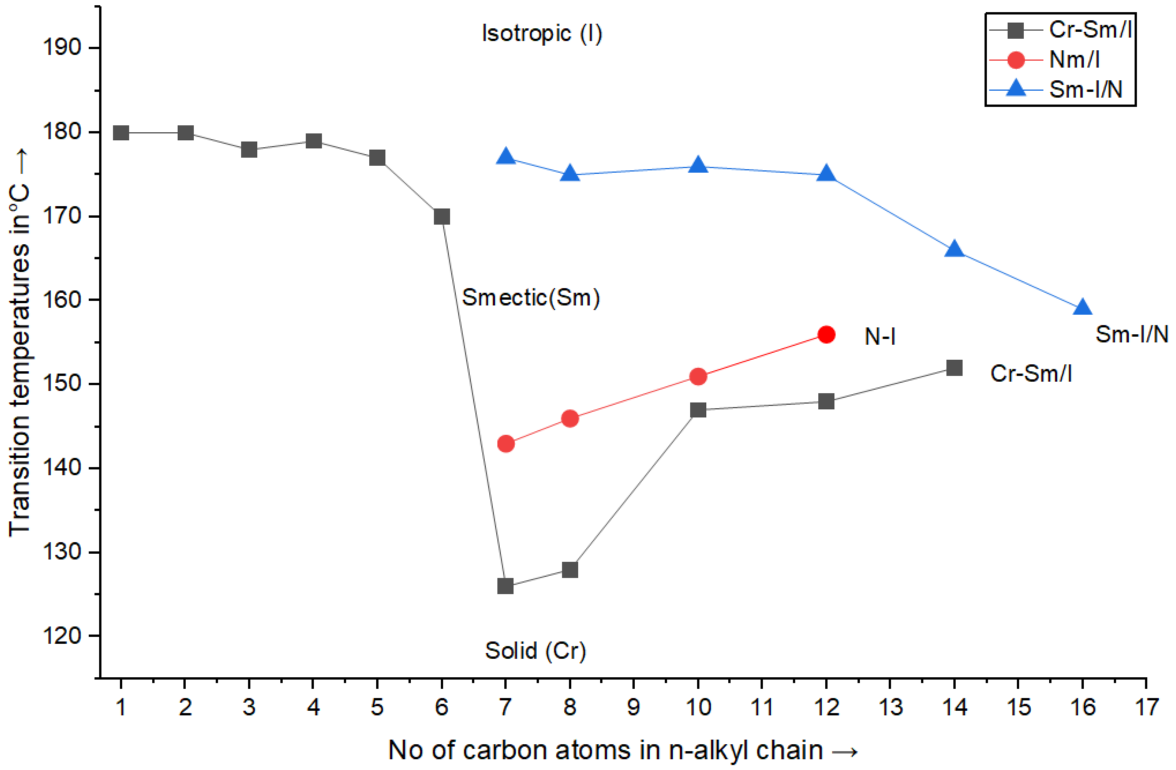

Figure 1. Phase behavior of homologues series.

The lateral methoxy groups increase molecular polarity, enhancing dipole–dipole interactions. DSC reveals higher ΔH for SmA→N transitions (ΔH ≈ 12–15 kJ mol^{-1}) in C_{10}–C_{16} compared to homologues without lateral methoxy, reflecting stronger cohesive forces and more ordered layered structures. The central azo bond introduces a rod-shaped geometry and enables photoisomerization. Nematic clearing temperatures increase by 5–8 °C relative to ester-only analogues, indicating that the planar –N=N– moiety enhances π-stacking. Entropy changes (ΔS ≈ 0.05–0.07 kJ mol^{-1} K^{-1}) at clearing point are lower, consistent with a more rigid core. Short tails (C_1–C_6) yield narrow nematic ranges (ΔT ≈ 10–15 °C) due to insufficient van der Waals interactions. Homologues C_7–C_{12} display broad nematic and smectic A phases (ΔT ≈ 25–40 °C) with SmC onset above 140 °C, owing to optimal chain interdigitation and lamellar packing.

Longer chains (C_{14}–C_{18}) slightly reduce clearing points while widening SmA ranges, attributable to increased chain flexibility and entropy. The measured enthalpy and entropy reflect a trade-off between core rigidity and tail freedom. Higher ΔH values for smectic transitions correlate with stronger layer formation in mid-length homologues, whereas elevated ΔS for long-chain compounds indicates enhanced disorder at phase boundaries. Present homologous series exhibits interesting mesomorphic behavior that can be correlated with molecular structure. The first six homologues (C1-C6) are non-mesomorphic, likely due to insufficient molecular length and inadequate anisotropic intermolecular interactions. Mesomorphism commences from the heptyloxy derivative (C7) and continues through the series, with both nematic and smectic phases observed, shown in Figure 1. The nematic phase appears in compounds C7-C12, characterized by orientational order without positional order. The smectic phase is observed in compounds C7-C16, indicating layered molecular arrangements. The coexistence of both phases in certain homologues (C7-C12) suggests polymorphic behavior, which is advantageous for applications requiring multiple phase transitions. The thermal stability of the nematic phase decreases slightly with increasing alkyl chain length, from 177°C (C7) to 159°C (C16), following typical behavior for homologous series where longer chains reduce intermolecular interactions between rigid cores. The smectic phase shows maximum thermal stability around C14 (152°C), indicating optimal balance between molecular length and intermolecular attractions.

4.2. Thermal Analysis (DSC)

DSC analysis was performed on selected compounds to validate POM observations and provide quantitative thermal data.

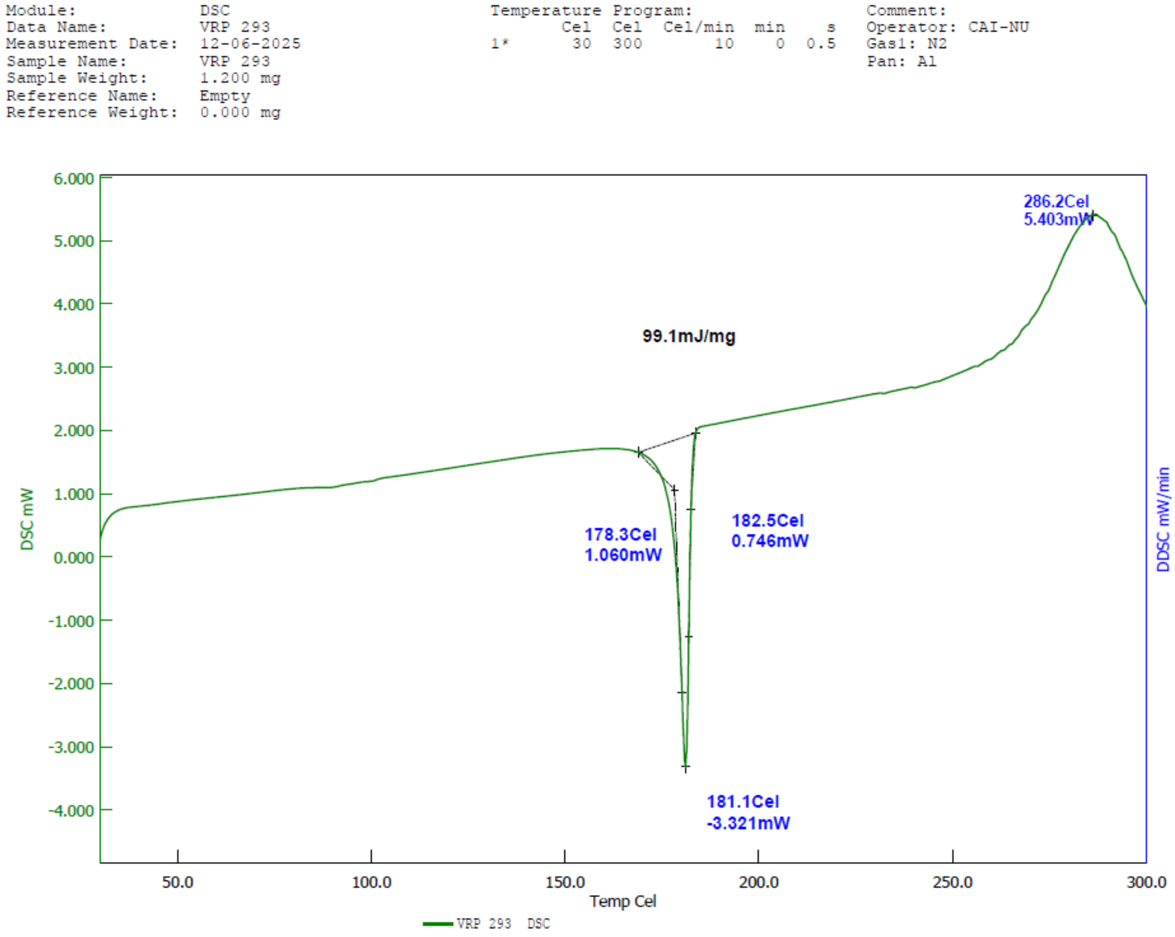

```
Module:             DSC                          Temperature Program:                   Comment:
Data Name:          VRP 293                             Cel   Cel  Cel/min   min    s   Operator: CAI-NU
Measurement Date:   12-06-2025                   1*      30   300       10     0  0.5   Gas1: N2
Sample Name:        VRP 293                                                             Pan: Al
Sample Weight:      1.200 mg
Reference Name:     Empty
Reference Weight:   0.000 mg
```

Figure 2. DSC data of octyloxy derivatives.

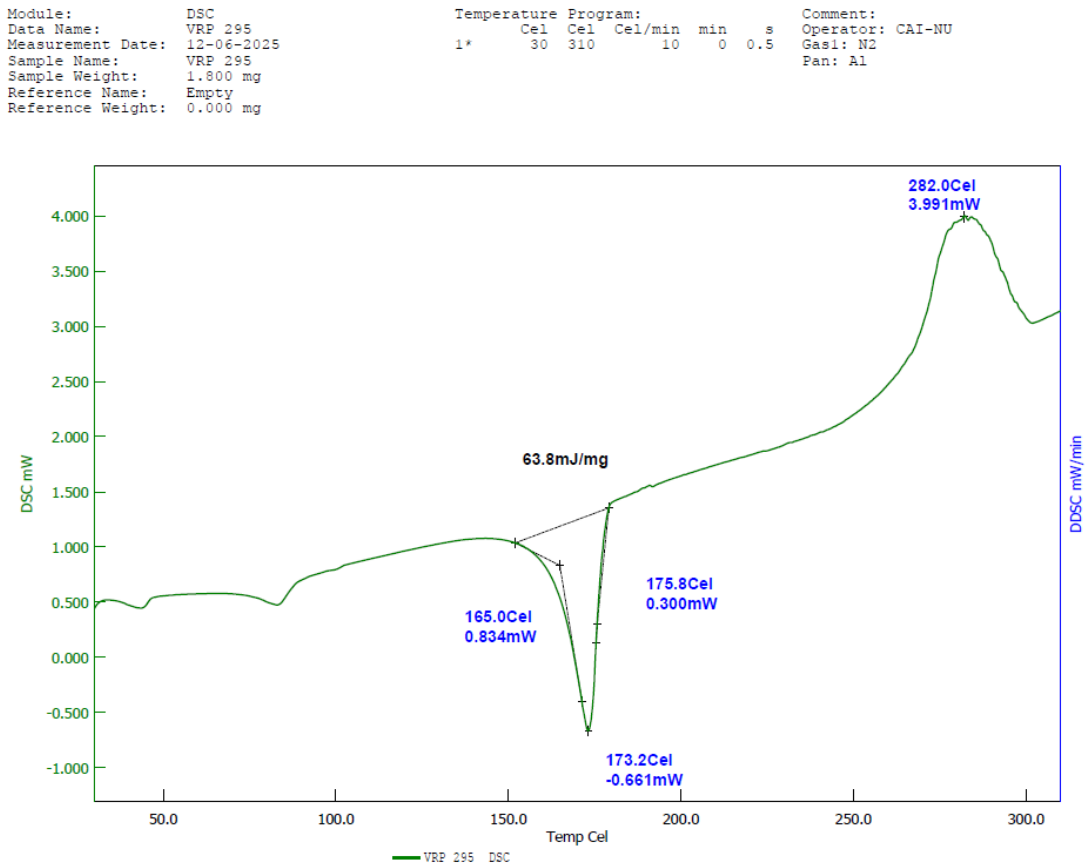

```
Module:             DSC                          Temperature Program:                 Comment:
Data Name:          VRP 295                           Cel   Cel  Cel/min  min    s      Operator: CAI-NU
Measurement Date:   12-06-2025                   1*    30   310       10    0  0.5      Gas1: N2
Sample Name:        VRP 295                                                            Pan: Al
Sample Weight:      1.800 mg
Reference Name:     Empty
Reference Weight:   0.000 mg
```

Figure 3. DSC data of dodecyloxy derivatives.

Thermograms confirmed the presence of distinct phase transitions corresponding to smectic-nematic and nematic-isotropic transitions shown in Figure 2 and Figure 3. The enthalpy changes associated with these transitions provide insights into the energy required for phase transitions and the stability of mesophases.

4.3. Optical Microscopy (POM)

POM investigations revealed characteristic textures associated with different mesophases:

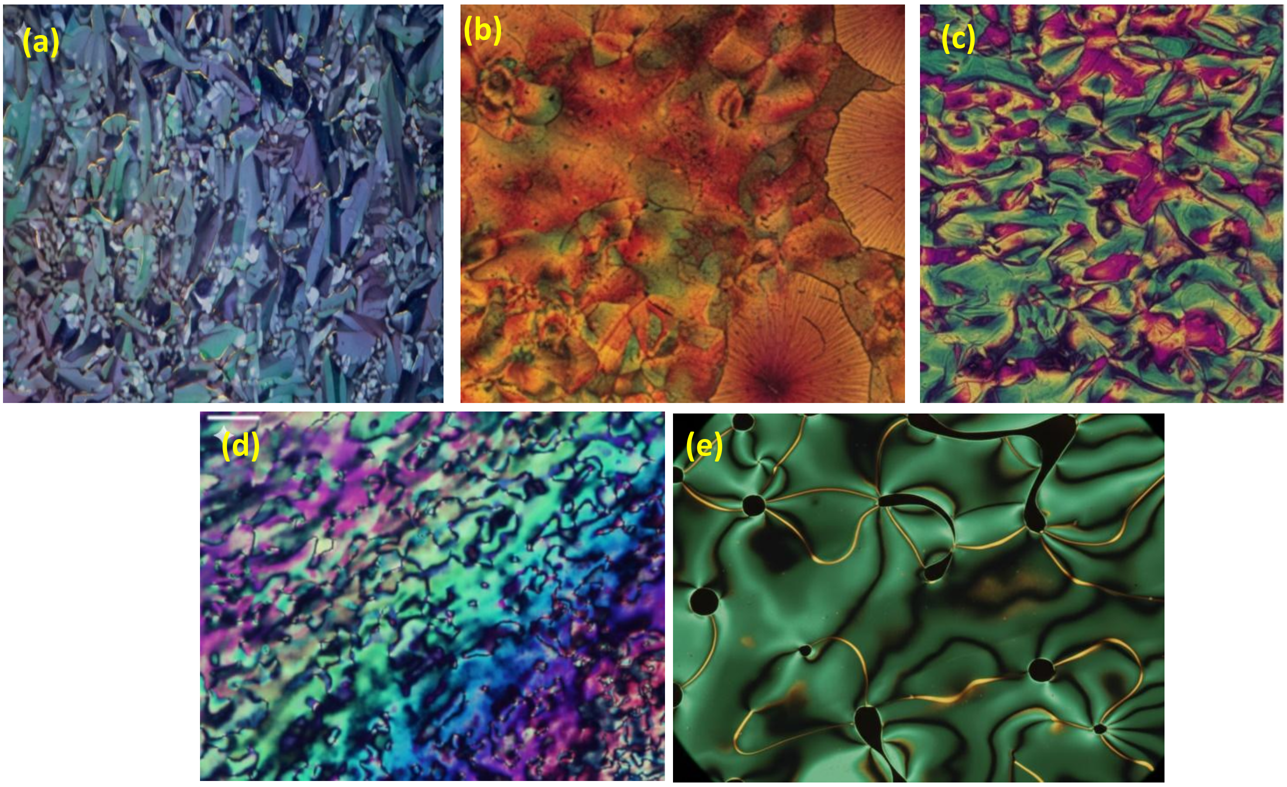

Figure 4. POM optical photomicrographs of (a) Smectic A (SmA) phase exhibited by C8 compound, (b) texture of the Smectic C (SmC) phase exhibited by C12 compound, (c) Smectic A (SmA) phase (focal-conic fan texture) exhibited by C14 compound, (d) Nematic (N) phase exhibited by C8 compound, (e) Nematic (N) phase (marble-like texture) exhibited by C10.

Nematic phase exhibited threaded and droplet textures typical of nematic liquid crystals, and Smectic phase displayed focal-conic and fan-shaped textures characteristic of Smectic A phases. The optical textures confirm the mesomorphic assignments and provide visual evidence for the liquid crystalline behavior of the synthesized compounds. To better understand the structure-property relationships, the mesomorphic properties of the present series were compared with structurally related compounds from literature. The incorporation of naphthalene units and methoxy substituents significantly influences the mesomorphic behavior compared to simpler azo-ester systems. Extended π-conjugation provided by the naphthalene ring enhances molecular polarizability and intermolecular interactions, contributing to the observed mesomorphic behavior. The methoxy substituents provide additional polar interactions while maintaining favorable molecular shape for liquid crystalline phases.

5. CONCLUSIONS

This investigation successfully established a novel homologous series of multi-ring azo-ester liquid crystals with well-defined structure-property relationships. The synthesized (2-(4'-n-alkoxy-3'-methoxybenzoyloxy)-naphthylazo-2''-methoxybenzenes) series (C_1-C_{18}) was prepared via efficient three-step synthesis (65-78% yields) and comprehensively characterized using spectroscopic and thermal analytical techniques. The systematic mesomorphic investigation revealed that compounds C_7-C_{18} exhibit robust liquid crystalline behavior, with C_7-C_{12} displaying dual nematic-smectic polymorphism. Nematic clearing temperatures range from 159-177°C while smectic transition temperatures span 126-152°C, demonstrating exceptional thermal stability. Short-chain homologues (C_1-C_6) lack sufficient molecular length for mesophase stabilization, while intermediate chains (C_7-C_{12}) provide optimal balance between core rigidity and terminal flexibility, yielding broad mesophase ranges (17-51°C). Longer chains (C_{14}-C_{18}) maintain robust smectic phases despite slightly reduced clearing temperatures.

The enhanced mesomorphic properties directly result from synergistic effects of the naphthalene core system (increased rigidity and π-π stacking), azo linkages (linear geometry and potential photochemical responsiveness), ester connections (thermal stability and dipolar interactions), and methoxy lateral substituents (enhanced intermolecular forces). The systematic dependence of thermal transitions on alkyl chain length follows predictable trends while revealing unique features of this molecular architecture. The successful integration of multiple functional elements within single molecular frameworks demonstrates effective molecular design strategies for advanced liquid crystalline materials. These compounds show promise for applications requiring high thermal stability and broad operating temperature ranges, including advanced displays and photonic devices. This work advances fundamental understanding of multi-ring mesogenic systems and establishes new design principles for next-generation liquid crystalline materials.

ACKNOWLEDGMENTS

The authors express sincere gratitude to the Department of Chemistry, Sheth P.T. Arts and Science College, Godhra, for providing essential research facilities and infrastructure support throughout this investigation. Special appreciation is extended to Dr. M.B. Patel, Principal, S.P.T. Arts & Science College, Godhra, for his continuous encouragement and administrative support that enabled the successful completion of this research program. Also, the invaluable technical assistance provided by the instrumentation facilities at various institutions for spectroscopic and thermal analysis. The authors are particularly grateful for access to advanced characterization techniques that enabled comprehensive materials evaluation.

References

[1] Reinitzer, F. Beiträge zur Kenntniss des Cholesterins. Monatsh. Chem. 1888, 9, 421–441.

[2] Gray, G. W. Molecular Structure and the Properties of Liquid Crystals; Academic Press: London, 1962.

[3] Kumar, S. Liquid Crystals: Experimental Study of Physical Properties and Phase Transitions; Cambridge University Press: Cambridge, 2001.

[4] Chandrasekhar, S. Liquid Crystals, 2nd ed.; Cambridge University Press: Cambridge, 1992.

[5] de Gennes, P. G.; Prost, J. The Physics of Liquid Crystals, 2nd ed.; Oxford University Press: Oxford, 1993.

[6] Dave, J. S.; Vora, R. A. In Liquid Crystals and Ordered Fluids; Johnson, J. F.; Porter, R. S., Eds.; Plenum Press: New York, 1970; pp 477–496.

[7] Furniss, B. S.; Hannaford, A. J.; Smith, P. W. G.; Tatchell, A. R. Vogel’s Textbook of Practical Organic Chemistry, 5th ed.; Longman: London, 1989.

[8] Beyer, H.; Walter, W. Lehrbuch der Organischen Chemie; S. Hirzel Verlag: Stuttgart, 1991.

[9] March, J. Advanced Organic Chemistry: Reactions, Mechanisms, and Structure, 4th ed.; Wiley: New York, 1992.

[10] Neises, B.; Steglich, W. Simple Method for the Esterification of Carboxylic Acids. Angew. Chem. Int. Ed. 1978, 17, 522–524.

[11] Kumar, G. S. Azo Functional Liquid Crystalline Polymers: An Update of Recent Research. Liq. Cryst. 2005, 32, 1089–1113.

[12] Matharu, A. S.; Jeeva, S.; Ramanujam, P. S. Liquid Crystals for Holographic Optical Data Storage. Chem. Soc. Rev. 2007, 36, 1868–1880.

[13] Yager, K. G.; Barrett, C. J. Novel Photo-Switching Using Azobenzene Functional Materials. J. Photochem. Photobiol. A 2006, 182, 250–261.

[14] Lagerwall, J. P. F.; Scalia, G. A New Era for Liquid Crystal Research: Applications of Liquid Crystals in Soft Matter Nano-, Bio- and Microtechnology. Curr. Appl. Phys. 2012, 12, 1387–1412.

[15] Tschierske, C. Development of Structural Complexity by Liquid-Crystal Self-assembly. Angew. Chem. Int. Ed. 2013, 52, 8828–8878.

[16] Fuhrmann, E.; Talbiersky, J. Synthesis of Alkyl Aryl Ethers by Catalytic Williamson Ether Synthesis with Weak Alkylation Agents. Org. Process Res. Dev. 2005, 9, 206–211.

[17] Patel, V. R.; Vyas, N. N.; Doshi, A. V. Synthesis and Mesomorphic Behavior of Novel Liquid Crystalline: 2-[4′-n-Alkoxy Benzoyloxy]-Naphthylazo-2″-Methoxy Benzenes. Mol. Cryst. Liq. Cryst. 2012, 569, 15–23.

[18] Chauhan, M. L.; Pandya, R. N.; Doshi, A. V. Synthesis and Mesomorphism of Novel Liquid Crystalline: p-(4′-n-Alkoxybenzoyloxy) Methyl Cinnamates. Mol. Cryst. Liq. Cryst. 2011, 548, 228–234. https://doi.org/10.1080/15421406.2011.591664.

[19] Patel, R. B.; Patel, V. R.; Doshi, A. V. Synthesis and Mesomorphism of Novel Liquid-Crystalline Isobutyl-p-(p′-n-Alkoxy Cinnamoyloxy) Cinnamates. Mol. Cryst. Liq. Cryst. 2012, 552, 3–9.

[20] Chauhan, S.; Patel, V. R. A Synthesis and Mesophase Behaviour of Homologous Series: 4-(4′-n-Alkoxyvanilloyloxy) Phenyl-azo-4″-ethylbenzoate with Terminal Ester Group as an Ethyl Carboxylate. WSN 2024, 191, 30–42.

[21] Hendrickson, J. B.; Wolf, W. A. Direct Introduction of the Diazo Function in Organic Synthesis. J. Org. Chem. 1968, 33, 3610–3618.

[22] Jordan, A.; Stoy, P.; Sneddon, H. F. A Solvent-Reagent Selection Guide for Steglich-Type Esterification of Carboxylic Acids. Green Chem. 2021, 23, 6405–6413.